NUCL SCI TECH (2018) 29:183
https://doi.org/10.1007/s41365-018-0517-7

Mean-field description of heavy-ion scattering at low energies and fusion

Dao T. Khoa[1] · Le Hoang Chien[1,2] · Do Cong Cuong[1] · Nguyen Hoang Phuc[1]

Received: 11 September 2018 / Revised: 18 October 2018 / Accepted: 31 October 2018 / Published online: 26 November 2018

Abstract The nuclear mean-field potential built up during the $^{12}C + ^{12}C$ and $^{16}O + ^{16}O$ collisions at low energies relevant for the carbon- and oxygen-burning processes is constructed within the double-folding model (DFM) using the realistic ground-state densities of ^{12}C and ^{16}O, and CDM3Yn density-dependent nucleon–nucleon (NN) interaction. The rearrangement term, indicated by the Hugenholtz–van Hove theorem for the single-particle energy in nuclear matter, is properly considered in the DFM calculation. To validate the use of the density-dependent NN interaction at low energies, an adiabatic approximation was suggested for the dinuclear overlap density. The reliability of the nucleus–nucleus potential predicted through this low-energy version of the DFM was tested in the optical model (OM) analysis of the elastic $^{12}C + ^{12}C$ and $^{16}O + ^{16}O$ scattering data at energies below 10 MeV/nucleon. These OM results provide a consistently good description of the elastic angular distributions and 90° excitation function. The dinuclear mean-field potential predicted by the DFM is further used to determine the astrophysical S factor of the $^{12}C + ^{12}C$ and $^{16}O + ^{16}O$ fusions in the barrier penetration model. Without any adjustment of the potential strength, our results reproduce the non-resonant behavior of the S factor of the $^{12}C + ^{12}C$ and $^{16}O + ^{16}O$ fusions very well over a wide range of energies.

Keywords Folding model · Elastic scattering · Fusion

1 Introduction

The $^{12}C + ^{12}C$ and $^{16}O + ^{16}O$ fusions at low energies, known as the carbon- and oxygen-burning processes, play a vital role in stellar nucleosynthesis [1, 2]. In massive stars with $M \gtrsim 8M_{\odot}$ where the electron degeneracy pressure is insufficient to prevent the gravitational collapse, a large accumulation of ^{12}C and ^{16}O ashes built up from the helium-burning phase starts to fuse together. In particular, the $^{12}C + ^{12}C$ fusion occurs at a temperature of $(0.6 - 1.0) \times 10^9$ K and matter density of approximately 10^6 g/cm^3 and yields ^{23}Na, ^{20}Ne, and ^{23}Mg for further burning stages during the stellar evolution. With a higher Coulomb barrier, the $^{16}O + ^{16}O$ fusion requires a temperature of $(1.5 - 2.7) \times 10^9$ K and densities of approximately $(2.6 - 6.7) \times 10^9$ g/cm^3 to synthesize ^{28}Si, ^{31}P, and ^{31}S. Owing to the important role of the $^{12}C + ^{12}C$ and $^{16}O + ^{16}O$ fusions in nuclear astrophysics, numerous studies have been conducted to investigate the fusion cross sections of these systems at low energies that are close to those relevant for the stellar nucleosynthesis [3–25].

In the hot stellar environment, the $^{12}C + ^{12}C$ and $^{16}O + ^{16}O$ fusions occur at energies well below the Coulomb barriers of these systems, i.e., around the Gamow peak of approximately 1.5 and 6.6 MeV for the $^{12}C + ^{12}C$ and

The present research has been supported, in part, by the National Foundation for Scientific and Technological Development (NAFOSTED Project No. 103.04-2017.317)

✉ Le Hoang Chien
lhchien@hcmus.edu.vn; chienlhphys@gmail.com

[1] Institute for Nuclear Science and Technology, VINATOM, 179 Hoang Quoc Viet, Hanoi, Vietnam

[2] Department of Nuclear Physics and Nuclear Engineering, Faculty of Physics and Engineering Physics, University of Science, VNU-HCM, 227 Nguyen Van Cu Street, District 5, Ho Chi Minh City, Vietnam

$^{16}O + ^{16}O$ systems, respectively. At such sub-barrier energies, the fusion cross section falls off exponentially, which makes the direct measurement of the fusion extremely difficult. Therefore, for the astrophysical simulations of the stellar nucleosynthesis, one usually needs to extrapolate the $^{12}C + ^{12}C$ and $^{16}O + ^{16}O$ fusion cross section to the low-energy region based on the experimental data measured at higher energies. However, uncertainties in such a procedure remain very significant [10] owing to the observed resonant structure of the fusion cross section [8, 11, 21] as well as the discrepancy between the data sets obtained from different measurements in the same energy range, such as discrepancy between the data of the $^{16}O + ^{16}O$ reaction obtained from the γ-ray and charged particle detection techniques [13, 14]. Thus, it is of significant interest to have a reliable theoretical prediction of the $^{12}C + ^{12}C$ and $^{16}O + ^{16}O$ fusion cross sections at the astrophysical energies. The theoretical studies to describe the fusion reactions so far are based mainly on the barrier penetration model (BPM) [26–28] using different models for the nucleus–nucleus potential [18, 19, 21–25]. The results of these studies show that the BPM description of the heavy-ion (HI) fusion depends strongly on the choice of the nucleus–nucleus interaction potential.

In general, the validity of a potential model for the description of the $^{12}C + ^{12}C$ or $^{16}O + ^{16}O$ interaction at the sub-Coulomb energies should first be tested in a consistent optical model (OM) analysis of elastic scattering at low energies. In fact, the measurements of the $^{12}C + ^{12}C$ and $^{16}O + ^{16}O$ elastic scattering and reaction have been taken over a wide range of energies during the last 40 years. However, it is not a simple task because of the ambiguity of the optical potential (OP) often observed in the OM studies of the elastic light HI scattering at low energies. In this regard, we remind the readers of the mean-field nature of the light HI interaction [29, 30]. For example, it was shown [30] that the mean-field potential built up from the $^{12}C + ^{12}C$ interaction smoothly matches the deep family of the real OP that provides a consistently good OM description of the elastic $^{12}C + ^{12}C$ scattering from the medium energies down to those near the Coulomb barrier. On the Hartree–Fock (HF) level, such a mean-field potential is readily obtained in the double-folding model (DFM) [29, 31–37]. At medium energies, the real OP given by the DFM was proven to account very well for the nuclear rainbow pattern observed in elastic light HI scattering [29, 35, 37]. In a smooth extrapolation of the mean-field potential to the low-energy region, the deep double-folded potential was shown [30] to provide a sufficient number of nodes in the relative-motion wave function, as indicated by the Pauli principle, and also provide a natural explanation of the low-energy $^{12}C + ^{12}C$ resonances in the cluster model of ^{24}Mg. This indicates that the DFM can be used as a realistic potential model for the description of the $^{12}C + ^{12}C$ and $^{16}O + ^{16}O$ fusions at the astrophysical energies. However, during the HI collision at such low energies, the nuclear medium is formed more or less adiabatically, and the nucleus–nucleus overlap density must be treated properly for the DFM calculation using a density-dependent nucleon–nucleon (NN) interaction. This may be the reason that simple versions of the DFM using some *density-independent* NN interaction are often used to calculate the nucleus–nucleus potential for the fusion study [7, 22].

Instead of the frozen density approximation (FDA) widely used in the DFM calculations at energies above 10 MeV/nucleon [34, 35, 37], we propose an adiabatic density approximation (ADA) for the dinuclear overlap density, which is used in the new version of the DFM [37], which properly includes the rearrangement term of the nuclear mean-field. The present (low-energy) version of the DFM is thereafter carefully tested in the OM analysis of elastic $^{12}C + ^{12}C$ and $^{16}O + ^{16}O$ scattering over a wide range of energies below 10 MeV/nucleon. The mean-field potential predicted by the DFM for both the $^{12}C + ^{12}C$ and $^{16}O + ^{16}O$ systems is further used in the BPM to determine the (non-resonant) energy-dependent astrophysical S factor for these two systems.

2 Mean-field-based DFM

We recall briefly that the nucleus–nucleus OP is evaluated in the DFM as an HF-type potential [31, 33–35] using some effective (energy- and density dependent) NN interactions $v(\rho, E)$. The direct term of the double-folded potential is local and evaluated at a given internuclear distance R using the ground-state (g.s.) densities of the two colliding nuclei as

$$V_{\rm D}(E,R) = \int \rho_a(\boldsymbol{r}_a)\rho_A(\boldsymbol{r}_A)v_{\rm D}(\rho,E,s)\mathrm{d}^3r_a\mathrm{d}^3r_A, \qquad \boldsymbol{s} = \boldsymbol{r}_A - \boldsymbol{r}_a + \boldsymbol{R}. \tag{1}$$

The antisymmetrization of the dinuclear system leads to the exchange term $V_{\rm EX}$ that is non-local in the coordinate space. A local Wentzel–Kramers–Brillouin (WKB)-based approximation is usually made [35] to obtain the exchange term in the following local form:

$$V_{\rm EX}(E,R) = \int \rho_a(\boldsymbol{r}_a, \boldsymbol{r}_a + \boldsymbol{s})\rho_A(\boldsymbol{r}_A, \boldsymbol{r}_A - \boldsymbol{s}) \times v_{\rm EX}(\rho, E, s) \exp\left(\frac{i\boldsymbol{K}(E,R).\boldsymbol{s}}{M}\right) {\rm d}^3 r_a {\rm d}^3 r_A, \quad (2)$$

where $\rho_{a(A)}(\boldsymbol{r}, \boldsymbol{r}')$ are the non-local g.s. density matrices; $M = aA/(a+A)$ is the recoil factor (or reduced mass number); a and A are the mass numbers of the projectile and target, respectively. The local relative momentum $K(E, R)$ is determined self-consistently as

$$K^2(E,R) = \frac{2\mu}{\hbar^2}[E - V(E,R) - V_{\rm C}(R)], \quad (3)$$

where μ is the reduced mass of the two nuclei and $V(E,R) = V_{\rm D}(E,R) + V_{\rm EX}(E,R)$ is the total real OP. The Coulomb potential $V_{\rm C}(R)$ is obtained by directly folding two uniform charge distributions [38], chosen to have the RMS charge radii $R_{\rm C} = 3.17$ and 3.54 fm for ^{12}C and ^{16}O, respectively.

For the effective NN interaction, in the present work, we have used the CDM3Yn density-dependent version [33] of the M3Y interaction based on the G-matrix elements of Paris potential [39]

$$v_{\rm D(EX)}(\rho, E, s) = g(E)F(\rho)v_{\rm D(EX)}(s). \quad (4)$$

The radial parts of the direct and exchange terms $v_{\rm D(EX)}(s)$ were maintained unchanged as given in terms of three Yukawas of the M3Y–Paris interaction [39]. The density-dependent functional $F(\rho)$ in Eq. (4) was first suggested in Ref. [33], with parameters chosen to properly reproduce the saturation properties of cold nuclear matter (NM) in the HF calculation (see Fig. 1). The $g(E)$ factor accounts effectively for the (in-medium) energy dependence of the CDM3Yn interaction (4) and is determined self-consistently [37] using the local relative momentum (3).

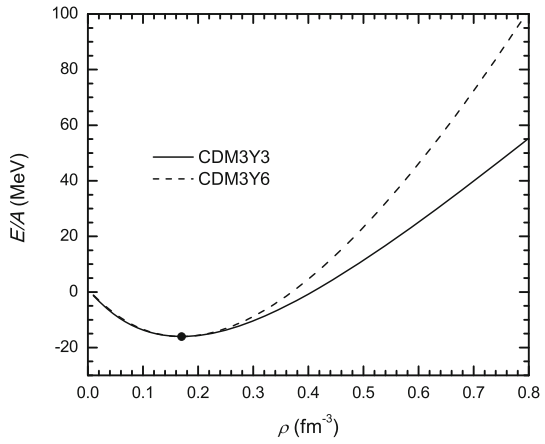

Fig. 1 Energy (per nucleon) of symmetric NM at different nucleon densities ρ given by the HF calculation using the CDM3Y3 and CDM3Y6 interactions (4), which provide the nuclear incompressibility $K = 217$ and 252 MeV, respectively, at the saturation point (solid circle)

In the HF calculation of the single-nucleon energy in NM using a density-dependent NN interaction, there appears naturally a rearrangement term (RT), which accounts for the rearrangement of the mean-field caused by the removal or addition of a single nucleon. The significant impact of the RT was shown experimentally in the direct nucleon transfer reactions at low energies [40]. In the same mean-field manner, the RT must appear in the HF-type folding model calculation of the nucleon–nucleus or nucleus–nucleus potential using an explicitly density-dependent NN interaction and single-nucleon wave functions of the projectile and target nucleons. This important aspect of the folding model has been investigated recently [37, 41], and it was shown that the contribution of the RT to the double-folded potential (1)–(2) can be accurately accounted for by adding a density-dependent correction term $\Delta F(\rho)$ to the density dependence $F(\rho)$ of the CDM3Yn interaction,

$$v_{\rm D(EX)}(\rho, E, s) = g(E)[F(\rho) + \Delta F(\rho)]v_{\rm D(EX)}(s) \quad (5)$$

must be used in the DFM calculation (1)–(2) of the nucleus–nucleus OP. The explicit parameters of the CDM3Yn interaction (4) with n = 3 and 6, and the corresponding RT correction (5) are given in Ref. [37]. In our approach, the contribution of the RT is added to the total double-folded potential as

$$V(E,R) = V_{\rm HF}(E,R) + V_{\rm RT}(E,R), \quad (6)$$

where $V_{\rm HF}$ and $V_{\rm RT}$ are the HF-type and rearrangement terms of the double-folded potential, respectively. The g.s. densities of ^{12}C and ^{16}O given by the no-core shell model [42] and Hartree–Fock–Bogoliubov (HFB) calculations [43], respectively, were used in the present work.

2.1 Adiabatic density approximation

As the strength and shape of the double-folded potential at small radii depend strongly on the dinuclear overlap density at these distances [35], an appropriate treatment of the overlap density is very important for the DFM calculation using a density-dependent NN interaction. The FDA, widely used so far in the double-folding calculation, assumes the sum of the two "frozen" g.s. densities for the overlap density ρ in Eq. (5).

$$\rho = \rho_1(\boldsymbol{r}_1) + \rho_2(\boldsymbol{r}_2). \quad (7)$$

The FDA was proven to be a reliable approximation at energies above 10 MeV/nucleon [31–33, 35, 36]. At low energies of the sub-barrier fusion, the dinuclear system

merges adiabatically into the compound nucleus [44–47] at decreasing internuclear distance R, and the FDA for a frozen overlap density is no longer valid. In an adiabatic scenario, the fusion time at low energies is sufficiently long for nucleons in the compound system to rearrange their initial states while maintaining the total energy of the system as low as possible. The ADA proposed here is similar to that suggested earlier in Refs. [48, 49], and the dinuclear overlap density evolves with the internuclear separation R as

$$\rho(r) = \begin{cases} 0.5\rho_c(r) & \exp\left[\ln\left(\frac{\rho_0(r)}{0.5\rho_c(r)}\right)\left(\frac{R}{R_{cut}}\right)\right] \\ & \text{if } R \leqslant R_{cut} \\ \rho_0(r) & \text{if } R > R_{cut}, \end{cases} \quad (8)$$

where R_{cut} is the grazing distance at which the two colliding nuclei start to rearrange themselves to form the compound nucleus; $\rho_0(r)$ and $\rho_c(r)$ are the g.s. densities of ^{12}C (or ^{16}O) nucleus and of the compound ^{24}Mg (or ^{32}S) nucleus, respectively. The $^{12}C + ^{12}C$ overlap densities given by the FDA and ADA are illustrated in Fig. 2. The chosen $R_{cut} = 6$ fm is close to the grazing distance suggested from the coupled channels study of fusion at sub-Coulomb energies [47]. It can be observed that the overlap density given by the FDA increases strongly at short distances, to approximately twice the central density of ^{12}C at $R = 0$, whereas that given by the ADA approaches the density of ^{24}Mg nucleus at small radii.

The impact of the two different treatments of the overlap density on the strength and shape of the double-folded $^{12}C + ^{12}C$ potential at the energy of approximately 7 MeV/nucleon obtained with the CDM3Y3 interaction is illustrated Fig. 3. As the overlap density given by the ADA is softer than that given by the FDA (see Fig. 2), the

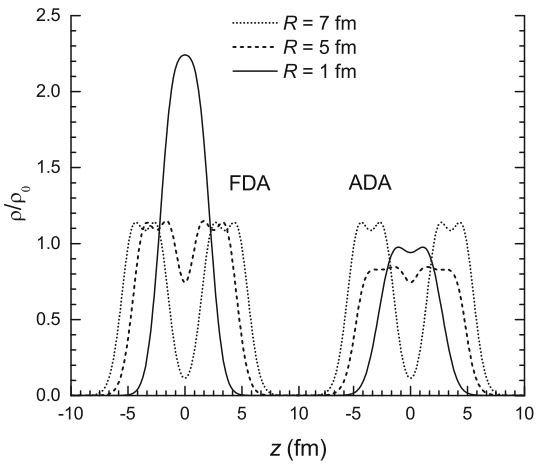

Fig. 2 $^{12}C + ^{12}C$ overlap density as a function of the internuclear separation R given by the FDA and ADA. The z axis is directed along the line connecting the centers of the two ^{12}C nuclei

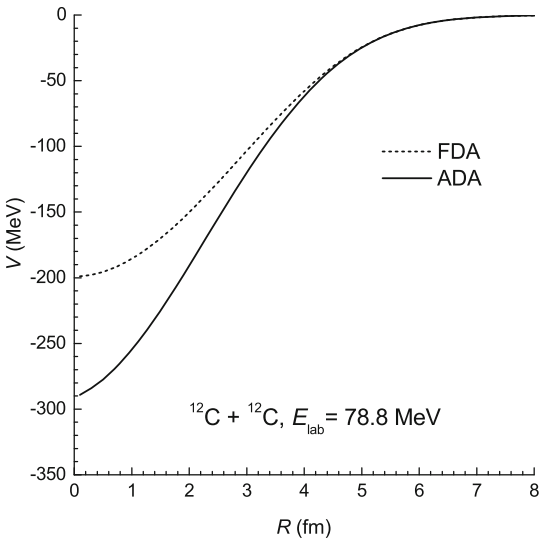

Fig. 3 Double-folded $^{12}C + ^{12}C$ potential at the incident energy of 78.8 MeV obtained with the CDM3Y3 interaction, and dinuclear overlap density given by the FDA (dash line) and ADA (solid line)

corresponding ADA double-folded potential is much deeper and has a larger slope in comparison with the FDA potential in the interior ($R < 6$ fm). Such a difference in the shape of the double-folded potential can be observed in the OM results for the elastic $^{12}C + ^{12}C$ scattering shown in Fig. 4.

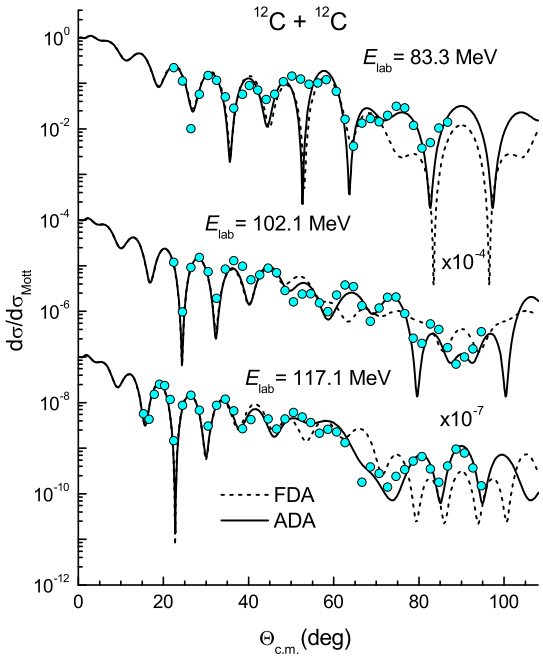

Fig. 4 OM description of the elastic $^{12}C + ^{12}C$ scattering at 83, 102, and 117 MeV given by the real double-folded OP using the FDA (dash line) and ADA (solid line) for the overlap density. The data were obtained from Ref. [52]

3 Results and discussion

3.1 Elastic $^{12}C + ^{12}C$ scattering and astrophysical *S* factor

The DFM should first be tested to verify its reliability in the OM study of elastic $^{12}C + ^{12}C$ scattering at low energies before using it as the potential model in the BPM calculation of the fusion cross section. For this purpose, the OM analysis of the elastic $^{12}C + ^{12}C$ scattering data at energies below 10 MeV/nucleon was performed using the CDM3Y3 double-folded potential as the real OP and Woods–Saxon (WS) potential as the imaginary OP, so that the total OP at the internuclear distance R is determined as

$$U(R) = V(E,R) + iW_V(R) + iW_D(R) + V_C(R), \quad (9)$$

$$\text{with } W_V(R) = \frac{-W_V}{1+\exp[(R-R_V)/a_V]}, \quad (10)$$

$$\text{and } W_D(R) = 4a_D \frac{d}{dR}\left\{\frac{W_D}{1+\exp[(R-R_D)/a_D]}\right\}. \quad (11)$$

The WS surface term (11) is optional and is used only in the case of the elastic $^{16}O + ^{16}O$ scattering. The WS parameters in (11) were obtained from the global OP of the $^{12}C + ^{12}C$ system [29, 50], with the potential strength slightly adjusted by the OM fit to the data under study (see Table 1). The Coulomb potential $V_C(R)$ is obtained by directly folding two uniform charge distributions [37] chosen to have the RMS charge radii $RC = 3.17$ and 3.54 fm for ^{12}C and ^{16}O ions, respectively. All the OM calculations were done using the code ECIS97 written by Raynal [51]. The OM results for the elastic $^{12}C + ^{12}C$ scattering at 83, 102, and 117 MeV given by the real CDM3Y3 double-folded OP using the FDA and ADA for the overlap density are compared with the measured data in Fig. 4. It can be observed that the folded potential obtained with the overlap density given by the FDA fails to account for the data measured at large angles, which are sensitive to the real OP at small distances [35] where the two approximations for the overlap density result in different potential strengths as shown in Fig. 3. Upon using a more realistic ADA for the overlap density, the double-folded potential provides a good description of the data at both forward and backward angles without any adjustment of the potential strength. The boson symmetry of the identical $^{12}C + ^{12}C$ system leads to the Mott oscillation of elastic cross section at large angles (see Fig. 4), which is peaked at $\theta_{c.m.} = 90^\circ$. Therefore, the elastic excitation function has been measured at 90° for this system at energies ranging from the Coulomb barrier to above 10 MeV/nucleon. A complex structure of the peaks and valleys in the measured $^{12}C + ^{12}C$ excitation function (see Fig. 5) was a challenge during the eighties, which was solved by McVoy and Brandan in a mean-field study of elastic $^{12}C + ^{12}C$ scattering [50] where they showed that the uneven structure in the 90° $^{12}C + ^{12}C$ excitation function is due to the evolution of the rainbow (Airy) pattern. In particular, the prominent minimum at 102 MeV is caused by the second Airy minimum passing through 90° at that energy [50]. As shown in Fig. 4, the elastic data measured at 102 MeV and two neighboring energies can be reproduced only by the real double-folded ADA potential.

These two versions of the real OP and the WS imaginary parts extrapolated from the global OP for elastic $^{12}C + ^{12}C$ scattering at the same energy range [29, 50] were used to calculate the 90° excitation function. We observed that only the ADA potential can reproduce the measured excitation function over a wide range of energies (see Fig. 5). Therefore, we conclude that the present version of the DFM provides a reliable prediction of the real OP for the $^{12}C + ^{12}C$ system at low energies and it should be a suitable potential model for the BPM study of the $^{12}C + ^{12}C$ fusion at the astrophysical energies.

In the BPM, the probability of the $^{12}C + ^{12}C$ fusion is determined by the tunnel effect that allows two ^{12}C nuclei to penetrate the Coulomb barrier at energies below the barrier height. Given the Q value of nearly 14 MeV, the $^{12}C + ^{12}C$ fusion can proceed through different channels involving the compound ^{24}Mg nucleus. While it is complicated to consider all these reaction channels properly in the coupled reaction channel calculation, the total $^{12}C + ^{12}C$ fusion cross section can be determined in the BPM as a coherent sum of all partial-wave contributions of the $^{12}C + ^{12}C$ transmission

Table 1 OM parameters in (9), (11), and (11) used in the folding analysis of the elastic $^{12}C + ^{12}C$, $^{16}O + ^{16}O$ scattering at energies considered in Figs. 4 and 8

System	E_{lab} (MeV)	W_V (MeV)	R_V (fm)	a_V (fm)	W_D (MeV)	R_D (fm)	a_D (fm)
$^{12}C + ^{12}C$	83.3	8.672	6.367	0.387	–	–	–
	102.1	14.326	5.584	0.591	–	–	–
	117.1	15.770	5.536	0.590	–	–	–
$^{16}O + ^{16}O$	48.5	8.254	5.351	0.282	0.708	7.823	0.221
	53.0	9.424	5.353	0.231	0.571	7.818	0.243
	63.0	14.170	5.373	0.380	3.428	6.997	0.354

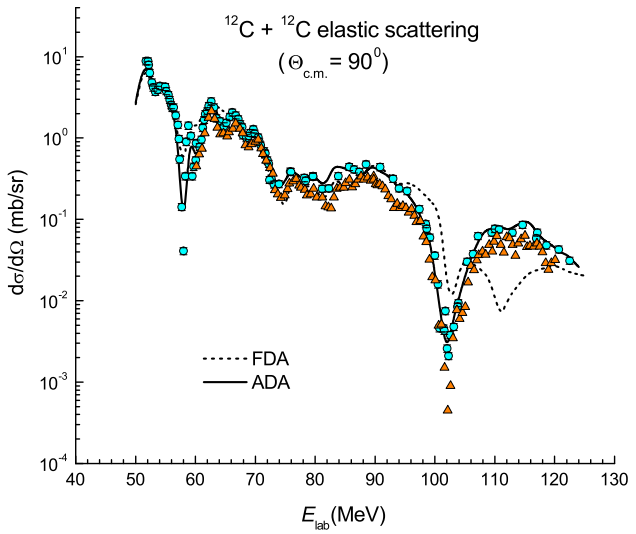

Fig. 5 OM description of the elastic $^{12}C + ^{12}C$ excitation function at $\theta_{c.m.} = 90^\circ$ given by the real double-folded OP based on the FDA (dash line) and ADA (solid line) of the overlap density. The data were obtained from Ref. [52–54]

$$\sigma fus = \frac{\pi}{k^2}\sum_{l=0}^{\infty}\left[1+(-1)^l\right](2l+1)T_l, \tag{12}$$

where k is the relative-motion momentum and l is the orbital angular momentum of the dinuclear system. The transmission coefficient T_l provides the probability of the two nuclei tunneling through the potential barrier built up from the attractive nuclear potential and repulsive Coulomb and centrifugal potentials as

$$V_l(R) = VN(R) + VC(R) + \frac{\hbar^2 l(l+1)}{2\mu R^2}. \tag{13}$$

The double-folded potential based on the ADA for the overlap density is used as the nuclear potential VN. For consistency, the same folded Coulomb potential V_C as that obtained in Eq. (3) is used to determine the total potential (13). To illustrate the impact of the potential model on the BPM results, we have also used two other models of the nuclear potential in the BPM study of the $^{12}C + ^{12}C$ fusion. The first one is the WS parameterization, denoted hereafter as the BRA potential, suggested for the OP of the $^{12}C + ^{12}C$ system at energies below 6 MeV/nucleon [55]. The other is the empirical potential parameterized to properly describe the g.s. band of ^{24}Mg in the $^{12}C + ^{12}C$ cluster model [56], denoted hereafter as the BH potential.

In general, the probability of fusion depends strongly on the height and location of the potential barrier. The double-folded (based on the ADA for the overlap density) potential provides the barrier height $V_{B0} = 6.2$ MeV at $R_{B0} = 7.8$ fm, which are consistent with the empirical values deduced [5] from the measured fusion data, $V_{B0} \approx 6.2 - 6.3$ MeV and $R_{B0} \approx 7.4 - 7.6$ fm. It can be observed in Fig. 6 that the double-folded potential provides a good description of the $^{12}C + ^{12}C$ fusion cross section over the entire energy range. The barrier heights and positions predicted by the BRA potential ($V_{B0} = 5.5$ MeV and $R_{B0} = 8.4$ fm) and the BH potential ($V_{B0} = 6.4$ MeV and $R_{B0} = 7.2$ fm) differ significantly from the empirical values. Consequently, the BPM results given by the BRA potential overestimate the fusion data in the energy region below 7 MeV, whereas those given by the BH potential underestimate the data (see Fig. 6).

As the fusion cross section decreases exponentially with the decrease in energy, it is more convenient to consider the astrophysical S factor of the fusion

$$S = E\sigma_{\rm fus}(E)\exp(2\pi\eta), \tag{14}$$

where the Sommerfeld parameter $\eta = Z_1Z_2e^2/\hbar v$, and v is the relative velocity of the dinuclear system. The astrophysical S factors obtained in the BPM with the three potential models are compared in Fig. 7 with the data and the empirical extrapolation by Fowler et al. [2] based on the data measured at higher energies. It can be observed that both the BRA and BH potentials fail to reproduce the data in the same way as discussed for the fusion cross section. The double-folded (based on the ADA for the overlap density) potential provides a good BPM description of the non-resonant behavior of the S factor over the entire energy range. The BPM results given by the double-folded potential are also reasonably consistent with the phenomenological S factor suggested by Fowler et al. except at the lowest energies where our mean-field results are slightly lower.

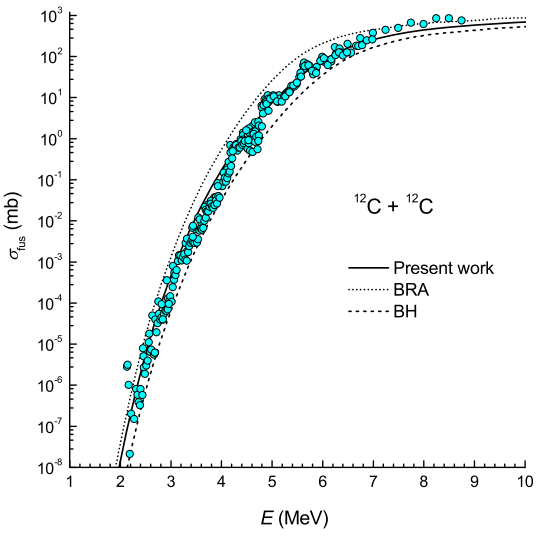

Fig. 6 BPM description of the $^{12}C + ^{12}C$ fusion cross section given by the double-folded (solid line), BRA [55] (dotted line), and BH [56] (dash line) potentials. The data were obtained from Refs. [5, 6, 8, 10]

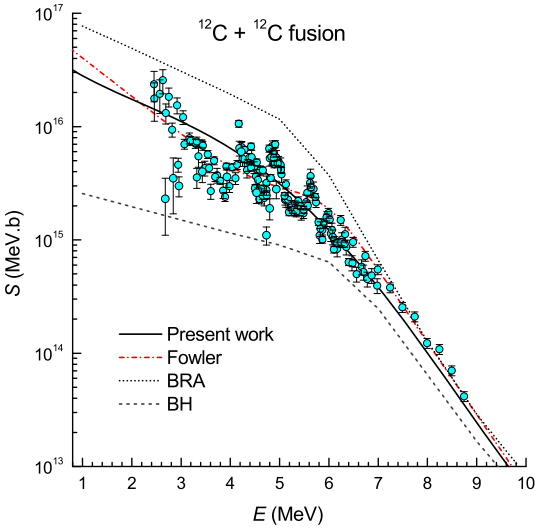

Fig. 7 Astrophysical S factor of the $^{12}C + ^{12}C$ fusion obtained in the BPM using the same potential models as those used to obtain the fusion cross sections shown in Fig. 6. The dashed–dotted curve is the phenomenological S factor extrapolated by Fowler et al. [2]. The data were obtained from Refs. [5, 6, 8, 10]

3.2 Results obtained for the $^{16}O + ^{16}O$ system

Given the higher Coulomb barrier, the $^{16}O + ^{16}O$ fusion occurs at higher temperature and densities compared with those of the stellar condition for the $^{12}C + ^{12}C$ fusion. So far, the S factor measured for the $^{16}O + ^{16}O$ fusion seems to be smooth, in contrast to that of the $^{12}C + ^{12}C$ fusion, which has uneven resonant behavior at low energies. Therefore, it is of interest to extend our mean-field approach to study the $^{16}O + ^{16}O$ fusion at energies of astrophysical interest. For this purpose, the $^{16}O + ^{16}O$ potential has been calculated in the DFM using the CDM3Y3 interaction and ADA for the overlap density, and the g.s. densities of ^{16}O and ^{32}S given by the Green Function Monte Carlo [57] and HFB [43] calculations, respectively. In the OM analysis, this version of DFM was used as the real OP, whereas the imaginary OP was assumed in the WS form with parameters given in Table 1. Without any renormalization of the potential strength, the OM results given by the double-folded potential account very well for the elastic $^{16}O + ^{16}O$ scattering data at low energies (see Fig. 8).

In the BPM study of the $^{16}O + ^{16}O$ fusion at energies around the Coulomb barrier, the double-folded potential (based on the ADA for the overlap density) provides a fairly good description of the measured S factor over a wide energy range, as shown in Fig. 9. The results given by the double-folded potential are also reasonably consistent with the phenomenological S factor suggested by Fowler et al. [2]. As in the $^{12}C + ^{12}C$ case, we have compared our

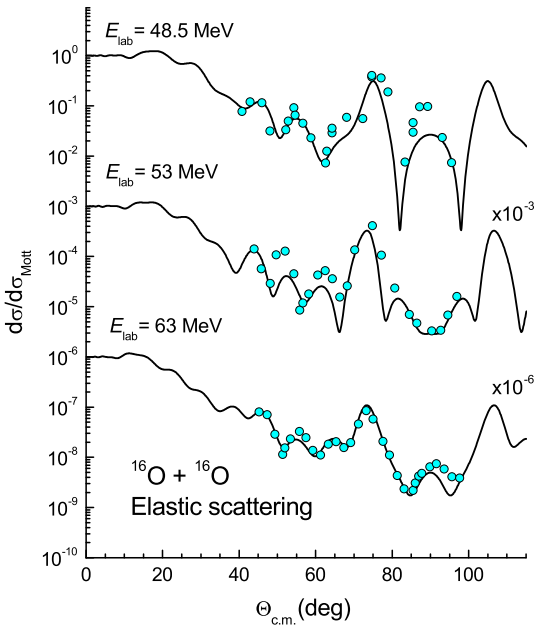

Fig. 8 OM description of the elastic $^{16}O + ^{16}O$ scattering at 48.5, 53, and 63 MeV given by the real double-folded OP based on the ADA for the overlap density. The data were obtained from Refs. [58, 59]

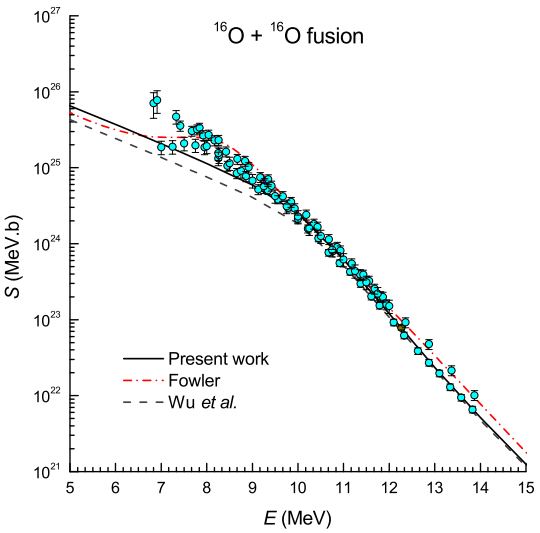

Fig. 9 Astrophysical S factor of the $^{16}O + ^{16}O$ fusion obtained in the BPM using the double-folded potential (solid line) and phenomenological OP suggested by Wu et al. [15] (dash line), in comparison with the data [13–16] and the empirical S factor extrapolated by Fowler et al. [2] from the measured data

mean-field results with those given by another potential model for the $^{16}O + ^{16}O$ fusion. That is, the phenomenological potential suggested by Wu et al. [15] for the study of the elastic $^{16}O + ^{16}O$ scattering at low energies and fusion has been used in the present BPM calculation. It can be observed in Fig. 9 that the phenomenological potential suggested by Wu et al. significantly underestimates the data

at sub-barrier energies. The results shown in Fig. 9 confirm the reliability of the low-energy version of the DFM in predicting the nucleus–nucleus potential for the BPM study of nuclear fusion.

The S factor given by the double-folded potential seems to slightly underestimate the data at low energies. A dynamic contribution from the coupled channel effects might well enhance the sub-barrier fusion cross section. This will be the subject of our future study.

4 Summary

The mean-field-based CDM3Y3 density-dependent interaction [33], well tested in the HF studies of nuclear matter [35] and nucleon mean-field potential [37, 41], has been used in the DFM approach to calculate the real OP for the elastic $^{12}C + ^{12}C$ and $^{16}O + ^{16}O$ scattering at low energies. With a realistic adiabatic approximation for the overlap density, the double-folded potential accounts very well for the observed oscillation and magnitude of the elastic $^{12}C + ^{12}C$ and $^{16}O + ^{16}O$ cross sections over a wide angular angle.

The present version of the DFM is further used to calculate the nuclear mean-field potential for the study of the astrophysical S factor of the $^{12}C + ^{12}C$ and $^{16}O + ^{16}O$ fusion in the BPM. Without any free parameter, the double-folded potential accounts very well for the non-resonant strength of the $^{12}C + ^{12}C$ and $^{16}O + ^{16}O$ astrophysical S factors. Our results are also consistent with those given by the phenomenological S factor extrapolated by Fowler et al. [2] from the data measured for these two systems. The OP given by the present version of the DFM can be used as a reliable input in the coupled reaction channels study of the $^{12}C + ^{12}C$ and $^{16}O + ^{16}O$ fusion, to explore explicitly the dynamic contribution from the coupled reaction channels to the total fusion cross section and astrophysical S factor at sub-barrier energies.

References

1. C. Iliadis, *Nuclear Physics of Stars* (Wiley-VCH Press, Weinheim, 2015)
2. W.A. Fowler, G.R. Caughlan, B.A. Zimmerman, Thermonuclear reaction rates, II. Ann. Rev. Astron. Astrophys. **13**, 69–112 (1975). https://doi.org/10.1146/annurev.aa.13.090175.000441
3. K.U. Kettner, H. Lorenz-Wirzba, C. Rolfs, The $^{12}C + ^{12}C$ reaction at subcoulomb energies (I). Z. Phys. A **298**, 65–75 (1980). https://doi.org/10.1007/BF01416030
4. W. Treu, H. Fröhlich, W. Galster et al., Total reaction cross section for $^{12}C + ^{12}C$ in the vicinity of the Coulomb barrier. Phys. Rev. C **22**, 2462–2464 (1980). https://doi.org/10.1103/PhysRevC.22.2462
5. E.F. Aguilera, P. Rosales, E. Martinez-Quiroz et al., New γ-ray measurements for $^{12}C + ^{12}C$ sub-Coulomb fusion: toward data unification. Phys. Rev. C **73**, 064601 (2006). https://doi.org/10.1103/PhysRevC.73.064601
6. L. Barrón-Palos, E.F. Aguilera, J. Aspiazu et al., Absolute cross sections measurement for the $^{12}C + ^{12}C$ system at astrophysically relevant energies. Nucl. Phys. A **779**, 318–332 (2006). https://doi.org/10.1016/j.nuclphysa.2006.09.004
7. L.R. Gasques, A.V. Afanasjev, E.F. Aguilera et al., Nuclear fusion in dense matter: reaction rate and carbon burning. Phys. Rev. C **72**, 025806 (2005). https://doi.org/10.1103/PhysRevC.72.025806
8. T. Spillane, F. Raiola, C. Rolfs et al., $^{12}C + ^{12}C$ fusion reactions near the Gamow energy. Phys. Rev. Lett. **98**, 122501 (2007). https://doi.org/10.1103/PhysRevLett.98.122501
9. B. Bucher, X.D. Tang, X. Fang et al., First direct measurement of $^{12}C\,(^{12}C\,,n)^{23}Mg$ at stellar energies. Phys. Rev. Lett. **114**, 251102 (2015). https://doi.org/10.1103/PhysRevLett.114.251102
10. C.L. Jiang, D. Santiago-Gonzalez, S. Almaraz-Calderon et al., Reaction rate for carbon burning in massive stars. Phys. Rev. C **97**, 012801(R) (2018). https://doi.org/10.1103/PhysRevC.97.012801
11. A. Tumino, C. Spitaleri, M. La Cognata et al., An increase in the $^{12}C + ^{12}C$ fusion rate from resonances at astrophysical energies. Nature **557**, 687–690 (2018). https://doi.org/10.1038/s41586-018-0149-4
12. A. Diaz-Torres, M. Wiescher, Characterizing the astrophysical S factor for $^{12}C + ^{12}C$ fusion with wave-packet dynamics. Phys. Rev. C **97**, 055802 (2018). https://doi.org/10.1103/PhysRevC.97.055802
13. H. Spinka, H. Winkler, Experimental determination of the total reaction cross section of the stellar nuclear reaction $^{16}O + ^{16}O$. Nucl. Phys. A **233**, 456–494 (1974). https://doi.org/10.1016/0375-9474(74)90469-2
14. G. Hulke, C. Rolfs, H.P. Trautvetter, Comparison of the fusion reactions $^{12}C + ^{20}Ne$ and $^{16}O + ^{16}O$ near the Coulomb barrier. Z. Phys. A **297**, 161–183 (1980). https://doi.org/10.1007/BF01421473
15. S.C. Wu, C.A. Barnes, Fusion and elastic scattering cross sections for the $^{16}O + ^{16}O$ reactions near the Coulomb barrier. Nucl. Phys. A **422**, 373–396 (1984). https://doi.org/10.1016/0375-9474(84)90523-2
16. J.G. Duarte, L.R. Gasques, J.R.B. Oliveira et al., Measurement of fusion cross sections for $^{16}O + ^{16}O$. J. Phys. G Nucl. Part. Phys. **42**, 065102 (2015). https://doi.org/10.1088/0954-3899/42/6/065102
17. C.L. Jiang, K.E. Rehm, B.B. Back, R.V.F. Janssens, Expectations for ^{12}C and ^{16}O induced fusion cross sections at energies of astrophysical interest. Phys. Rev. C **75**, 015803 (2007). https://doi.org/10.1103/PhysRevC.75.015803
18. VYu. Denisov, N.A. Pilipenko, Fusion of deformed nuclei: $^{12}C + ^{12}C$. Phys. Rev. C **81**, 025805 (2010). https://doi.org/10.1103/PhysRevC.81.025805
19. M. Notani, H. Esbensen, X. Fang et al., Correlation between the $^{12}C + ^{12}C$, $^{12}C + ^{13}C$, and $^{13}C + ^{13}C$ fusion cross sections. Phys. Rev. C **85**, 014607 (2012). https://doi.org/10.1103/PhysRevC.85.014607
20. C.L. Jiang, B.B. Back, H. Esbensen et al., Origin and consequences of $^{12}C + ^{12}C$ fusion resonances at deep sub-barrier energies. Phys. Rev. Lett. **110**, 072701 (2013). https://doi.org/10.1103/PhysRevLett.110.072701
21. M. Assunção, P. Descouvemont, Role of the Hoyle state in $^{12}C + ^{12}C$ fusion. Phys. Lett. B **723**, 355–359 (2013). https://doi.org/10.1016/j.physletb.2013.05.030

22. A.A. Aziz, N. Yusof, M.Z. Firihu, H.A. Kassim, Reliability of the double-folding potential for fusion cross sections of light systems. Phys. Rev. C **91**, 015811 (2015). https://doi.org/10.1103/PhysRevC.91.015811
23. H. Esbensen, Coupled-channels calculations of ^{16}O + ^{16}O fusion. Phys. Rev. C **77**, 054608 (2008). https://doi.org/10.1103/PhysRevC.77.054608
24. G. Kocak, M. Karakoc, I. Boztosun, A.B. Balantekin, Effects of α-cluster potentials for the ^{16}O + ^{16}O fusion reaction and *S* factor. Phys. Rev. C **81**, 024615 (2010). https://doi.org/10.1103/PhysRevC.81.024615
25. C. Simenel, R. Keser, A.S. Umar, V.E. Oberacker, Microscopic study of ^{16}O + ^{16}O fusion. Phys. Rev. C **88**, 024617 (2013). https://doi.org/10.1103/PhysRevC.88.024617
26. C.Y. Wong, Interaction barrier in charged-particle nuclear reactions. Phys. Rev. Lett. **31**, 766–769 (1973). https://doi.org/10.1103/PhysRevLett.31.766
27. K. Hagino, N. Takigawa, Subbarrier fusion reactions and many-particle quantum tunneling. Prog. Theor. Phys. **128**, 1061–1106 (2012). https://doi.org/10.1143/PTP.128.1061
28. B.B. Back, H. Esbensen, C.L. Jiang, K.E. Rehm, Recent developments in heavy-ion fusion reactions. Rev. Mod. Phys. **86**, 317–360 (2014). https://doi.org/10.1103/RevModPhys.86.317
29. M.E. Brandan, G.R. Satchler, The interaction between light heavy-ions and what it tells us. Phys. Rep. **285**, 143–243 (1997). https://doi.org/10.1016/S0370-1573(96)00048-8
30. Y. Kondō, M.E. Brandan, G.R. Satchler, Shape resonances and deep optical potentials: a mean-field description of ^{12}C + ^{12}C scattering at low energies. Nucl. Phys. A **637**, 175–200 (1998). https://doi.org/10.1016/S0375-9474(98)00212-7
31. G.R. Satchler, W.G. Love, Folding model potentials from realistic interactions for heavy-ion scattering. Phys. Rep. **55**, 183–254 (1979). https://doi.org/10.1016/0370-1573(79)90081-4
32. D.T. Khoa, W. von Oertzen, H.G. Bohlen, Double-folding model for heavy-ion optical potential: revised and applied to study ^{12}C and ^{16}O elastic scattering. Phys. Rev. C **49**, 1652–1668 (1994). https://doi.org/10.1103/PhysRevC.49.1652
33. D.T. Khoa, G.R. Satchler, W. von Oertzen, Nuclear incompressibility and density dependent *NN* interactions in the folding model for nucleus–nucleus potentials. Phys. Rev. C **56**, 954–969 (1997). https://doi.org/10.1103/PhysRevC.56.954
34. D.T. Khoa, G.R. Satchler, Generalized folding model for elastic and inelastic nucleus–nucleus scattering using realistic density dependent nucleon-nucleon interaction. Nucl. Phys. A **668**, 3–41 (2000). https://doi.org/10.1016/S0375-9474(99)00680-6
35. D.T. Khoa, W. von Oertzen, H.G. Bohlen, S. Ohkubo, Nuclear rainbow scattering and nucleus-nucleus potential. J. Phys. G **34**, R111–R164 (2007). https://doi.org/10.1088/0954-3899/34/3/R01
36. D.T. Khoa, α-nucleus optical potential in the double-folding model. Phys. Rev. C **63**, 034007 (2001). https://doi.org/10.1103/PhysRevC.63.034007
37. D.T. Khoa, N.H. Phuc, D.T. Loan, B.M. Loc, Nuclear mean field and double-folding model of the nucleus-nucleus optical potential. Phys. Rev. C **94**, 034612 (2016). https://doi.org/10.1103/PhysRevC.94.034612
38. J.E. Poling, E. Norbeck, R.R. Carlson, Elastic scattering of lithium by ^{9}Be , ^{10}B , ^{12}C , ^{13}C , ^{16}O , and ^{28}Si from 4 to 63 MeV. Phys. Rev. C **13**, 648–660 (1976). https://doi.org/10.1103/PhysRevC.13.648
39. N. Anantaraman, H. Toki, G.F. Bertsch, An effective interaction for inelastic scattering derived from the Paris potential. Nucl. Phys. A **398**, 269–278 (1983). https://doi.org/10.1016/0375-9474(83)90487-6
40. P.E. Hodgson, Nucleon removal and rearrangement energies. Rep. Prog. Phys. **38**, 847–902 (1975). https://doi.org/10.1088/0034-4885/38/7/002
41. D.T. Loan, B.M. Loc, D.T. Khoa, Extended Hartree-Fock study of the single-particle potential: the nuclear symmetry energy, nucleon effective mass, and folding model of the nucleon optical potential. Phys. Rev. C **92**, 034304 (2015). https://doi.org/10.1103/PhysRevC.92.034304
42. M. Gennari, M. Vorabbi, A. Calci, P. Navrátil, Microscopic optical potentials derived from ab initio translationally invariant nonlocal one-body densities. Phys. Rev. C **97**, 034619 (2018). https://doi.org/10.1103/PhysRevC.97.034619
43. S. Goriely, M. Samyn, J.M. Pearson, Further explorations of Skyrme–Hartree–Fock–Bogoliubov mass formulas. VII. Simultaneous fits to masses and fission barriers. Phys. Rev. C **75**, 064312 (2007). https://doi.org/10.1103/PhysRevC.75.064312
44. K. Siwek-Wilczýnska, J. Wilczýnski, Nucleus-nucleus fusion energy thresholds and the adiabatic fusion potential. Phys. Rev. C **64**, 024611 (2001). https://doi.org/10.1103/PhysRevC.64.024611
45. T. Ichikawa, K. Hagino, A. Iwamoto, Signature of smooth transition from sudden to adiabatic states in heavy-ion fusion reactions at deep sub-barrier energies. Phys. Rev. Lett. **103**, 202701 (2009). https://doi.org/10.1103/PhysRevLett.103.202701
46. Y. Taniguchi, Y. Kanada-Enýo, T. Suhara, Adiabatic internuclear potentials obtained by energy variation with the internuclear-distance constraint. Prog. Theor. Exp. Phys. **2013**, 043D04 (2013). https://doi.org/10.1093/ptep/ptt002
47. T. Ichikawa, Systematic investigations of deep sub-barrier fusion reactions using an adiabatic approach. Phys. Rev. C **92**, 064604 (2015). https://doi.org/10.1103/PhysRevC.92.064604
48. I. Reichstein, F.B. Malik, Dependence of ^{16}O + ^{16}O potential on the density ansatz. Phys. Lett. B **37**, 344–346 (1971). https://doi.org/10.1016/0370-2693(71)90197-3
49. N. Ohtsuka, R. Linden, A. Faessler, F.B. Malik, Real and imaginary parts of the microscopic optical potential between nuclei in the sudden and adiabatic approximation and its application to medium energy ^{12}C + ^{12}C scattering. Nucl. Phys. A **465**, 550–572 (1987). https://doi.org/10.1016/0375-9474(87)90364-2
50. K.W. McVoy, M.E. Brandan, The 90° excitation function for elastic ^{12}C + ^{12}C scattering: the importance of Airy elephants. Nucl. Phys. A **542**, 295–309 (1992). https://doi.org/10.1016/0375-9474(92)90218-9
51. J. Raynal, Computing as a Language of Physics, IAEA, Vienna p.75 (1972); coupled-channel code ECIS97 (unpublished)
52. R.G. Stokstad, R.M. Wieland, G.R. Satchler et al., Elastic and inelastic scattering of ^{12}C by ^{12}C from $E_{\mathrm{c.m.}} = 35 - 63$ MeV . Phys. Rev. C **20**, 655-669 (1979). https://doi.org/10.1103/PhysRevC.20.655
53. A. Morsad, F. Haas, C. Beck, R.M. Freeman, Detailed energy dependence of the elastic and inelastic ^{12}C + ^{12}C scattering between 5 and 10 MeV/nucleon. Z. Phys. A **338**, 61–65 (1991). https://doi.org/10.1007/BF01279115
54. W. Reilly, R. Wieland, A. Gobbi et al., A comparative study of the elastic scattering in the ^{12}C , ^{14}N and ^{16}O identical-particle systems. Nuov. Cim. A **13**, 897–912 (1973). https://doi.org/10.1007/BF02804157
55. M.E. Brandan, M. Rodrguez-Villafuerte, A. Ayala, ^{12}C + ^{12}C elastic scattering analysis above $E/A = 6$ MeV using deep real potentials. Phys. Rev. C **41**, 1520–1529 (1990). https://doi.org/10.1103/PhysRevC.41.1520
56. B. Buck, P.D.B. Hopkins, A.C. Merchant, A ^{12}C + ^{12}C cluster model of ^{24}Mg . Nucl. Phys. A **513**, 75–114 (1990). https://doi.org/10.1016/0375-9474(90)90344-L

57. S.C. Pieper, R.B. Wiringa, V.R. Pandharipande, Variational calculation of the ground state of ^{16}O . Phys. Rev. C **46**, 1741–1756 (1992). https://doi.org/10.1103/PhysRevC.46.1741
58. R.H. Siemssen, J.V. Maher, A. Weidinger, D.A. Bromley, Excitation-function structure in ^{16}O + ^{16}O scattering. Phys. Rev. Lett. **19**, 369–372 (1967). https://doi.org/10.1103/PhysRevLett.19.369
59. J.V. Maher, M.W. Sachs, R.H. Siemssen et al., Nuclear interaction of oxygen with oxygen. Phys. Rev. **188**, 1665–1683 (1969). https://doi.org/10.1103/PhysRev.188.1665